

(Plasticized) Polylactide/clay nanocomposite textile: thermal, mechanical, shrinkage and fire properties

Samuel Solarski · Fatma Mahjoubi · Manuela Ferreira · Eric Devaux ·
Pierre Bachelet · Serge Bourbigot · René Delobel · Philippe Coszach ·
Marius Murariu · Amália Da Silva Ferreira · Michael Alexandre ·
Philippe Degee · Philippe Dubois

Received: 30 March 2006 / Accepted: 1 September 2006 / Published online: 21 March 2007
© Springer Science+Business Media, LLC 2007

Abstract Various quantities of Cloisite[®] 30B (from 1% to 4% in weight) have been added to a polylactide matrix by melt blending to produce polylactide-based nanocomposites. Then, these blends have been melt-spun to produce multifilaments yarns. It is demonstrated that it is necessary to use a plasticizer to spin a blend with 4% in weight of Cloisite[®] 30B. The properties of these yarns have been studied (dispersion of the clay, thermal, mechanical and shrinkage properties). A decrease of the tensile properties is observed when the quantity of Cloisite[®] 30B increases, but an improvement of the thermal and shrinkage properties is highlighted. These multifilaments have been knitted and the flammability studied using cone calorimeter at 35 kW/m². A strong decrease, up to 38%, of the heat release rate has been measured.

Introduction

Poly(lactide) (PLA) is a biodegradable polymer, which can be spun to produce fibers. It is very interesting because PLA can be synthesized from renewable resources and it represents an interesting way to replace petroleum-based polymer. Different ways are available to spin PLA [1]. They can be obtained through a solution spinning process [2–8], a high-speed melt-spinning process [9–11] or through melt spinning drawing process [12–17].

One way to improve the properties of a polymeric material is to incorporate nanofillers like smectite clays, and more particularly montmorillonite (MMT). MMT is characterized by negatively charged aluminosilicate layers bounded by electrostatic forces via alkaline cations, such as sodium cations or ammonium cations (in organomodified MMT) located in the interlayer space. This kind of blend is called polymer-layered silicate nanocomposite, and their properties (thermal, mechanical, flammability, barrier...) can be strongly improved at low filler level (generally under 5% in weight) [18, 19]. Different kinds of nanocomposites can be obtained depending on the dispersion of the clay into the polymer matrix. If the polymer chains are located between the silicate layers, the structure is intercalated. If the silicate layers are fully delaminated in the matrix polymer, the structure is exfoliated. To check the dispersion of MMT in a polymer matrix, X-ray diffraction (XRD) and transmission electron microscopy (TEM) are generally used [20]. It is also possible to investigate the dispersion of clay using nuclear magnetic resonance (NMR). NMR can quantify the degree of dispersion of the clay, contrary to XRD and TEM, which give information about the kind of structure, but remain generally qualitative [21].

S. Solarski · F. Mahjoubi · M. Ferreira (✉) ·
E. Devaux
Laboratoire de Génie et Matériaux Textiles (GEMTEX), UPRES
EA2461, Ecole Nationale Supérieure des Arts et Industries
Textiles (ENSAIT), BP 30329, 59056 Roubaix Cedex 01, France
e-mail: manuela.ferreira@ensait.fr

P. Bachelet · S. Bourbigot · R. Delobel
Laboratoire Procédés d'Élaboration des Revêtements
Fonctionnels (PERF), LSPES UMR 8008, École Nationale
Supérieure de Chimie de Lille (ENSCL), BP 90108, 59652
Villeneuve d'Ascq Cedex, France

P. Coszach
Galactic s.a, Place d'Escanaffles 23, 7760 Escanaffles, Belgium

M. Murariu · A. Da Silva Ferreira · M. Alexandre ·
P. Degee · P. Dubois
Service des Matériaux Polymères et Composites (SMPC),
University of Mons-Hainaut, Place du Parc 20, 7000 Mons,
Belgium

Several articles comment the way to disperse clay into PLA, the improvement of the PLA properties, and the kind of structure obtained. In order to nanodisperse the clay in PLA, two main techniques are used: the solution-intercalation [22, 23], and the melt-blending processes [24–28]. Generally, an intercalated structure is obtained using an organomodified MMT (e.g., MMT modified by an alkyl ammonium cation bearing hydroxyl functions such as the commercial MMT Cloisite®30B hereafter called C30B, available from Southern Clays Products, US). The interactions between the carbonyl functions of PLA chains and hydroxyl functions of the alkyl ammonium surfactants surface-covering MMT nanoplatelets seem to improve the dispersion of this organo-clay in a PLA matrix, contrary to other kinds of MMT without hydroxyl functions on the surfactant [22, 24–27]. An original way to obtain a good dispersion of clay in a PLA matrix is the in situ coordination-insertion polymerization [29]. The growing polymer chains are directly grafted on the surface of the organo-clay, the surfactant of which containing hydroxyl functions that promote the complete delamination of the silicate layers. The PLA nanocomposites are characterized by an increase of the crystallization rate but also by a decrease of the ability to crystallize, so by a lower melting enthalpy compared to pristine PLA [22, 25, 29]. But the clay does not seem to influence the glass transition temperature (T_g) of PLA [22, 25, 29]. An improvement of the thermal stability can be obtained, especially when C30B is used [24, 30].

The effects of plasticizer on the properties of PLA [31–36] and PLA [24, 28, 30] nanocomposites have also been largely investigated. Several plasticizers can be used to modify the properties of PLA: poly(ethylene glycol) with different molecular weight [24, 28, 30–32, 35, 36], some citrate derivatives [31–34], glycerol and oligomeric lactic acid [31]. The addition of a suitable plasticizer into a PLA matrix generally decreases the T_g and the melting temperature (T_m), the molecular mobility being improved [31–33]. It decreases also the modulus and the tensile strength, but it increases the elongation at break [31, 32].

The aim of this paper is to use organo-clays to reinforce some properties of PLA filaments and related textile structure. The use of a polymeric matrix to produce a nanocomposite multifilament yarn has been described for the first time in 2002 by Bourbigot et al. [37]. The matrix used was polyamide-6 (PA6) reinforced with C30B. The flammability of knitted structure made with PA6 and PA6/C30B was investigated using cone calorimeter and a strong decrease of the heat release rate was measured. The present paper proposes a method to produce PLA organo-clay nanocomposites filaments. In a first time, some properties of the PLA organo-clay nanocomposites, such as the kind of nanocomposite structure, the kinetics crystallization and

the thermal stability are investigated to study the influence of the organo-clay. Then, the thermal, mechanical and shrinkage properties of the nanocomposite multifilament yarns are also examined. The fire behavior of the PLA nanocomposite knitted fabrics is finally discussed using a cone calorimeter.

Experimental

Material

Poly(L,L-lactide) (PLA) sample-commercial name “GALASTIC”, was supplied by Galactic S.A. and used as biodegradable polyester matrix (characteristics of this PLA are as follows: Mn(PLA): 74500, residual monomer: 0.18%, relative viscosity: 3.96, D-isomer: 4.3%. Before processing, PLA was dried 12 h at 80 °C.

The additive used for the preparation of the PLA nanocomposites is C30B supplied by Southern Clay Products (USA). The surfactant of the C30B is a methyl tallow alkyl bis-2-hydroxyethyl quaternary ammonium cation. C30B is delivered in the shape of a fine powder. The plasticizer used is dioctyl adipate (DOA, $C_{22}H_{42}O_4$, $M_w = 370.57 \text{ g mol}^{-1}$) supplied by Acros Organics. This plasticizer was chosen because of its high thermal stability.

Nanocomposite preparation

PLA nanocomposites are prepared through melt-direct intercalation using a conventional polymer extrusion process. PLA pellets with 1%, 2%, 3% and 4% in weight of C30B (noted N1_p, N2_p, N3_p and N4_p) are blended using a counter-rotating extruder (Brabender DSK, diameter of screw = 41 mm, $L/D = 7.5$). The temperatures of the three zones are 175 °C/180 °C/185 °C. The rotation speed of the screws is maintained at 25 rpm. The extrudate is then pelletized.

Plasticized PLA nanocomposites are also prepared through melt-direct intercalation by using a conventional polymer extrusion process. PLA pellets with 4 wt.% C30B and 10 wt. % DOA (noted pN4_p) is blended using co-rotating extruder (Thermo Haake, diameter of screw = 16 mm, $L/D = 25$). The temperatures of the five zones are 140 °C/160 °C/170 °C/180 °C/190 °C. The rotation speed is maintained at 150 rpm. PLA and C30B are incorporated in a first feeding zone. The plasticizer is incorporated in the second feeding zone located in the middle of the extruder (see Fig. 1). This method was adopted to ensure the intercalation of PLA between the silicate layers of C30B in a first time, and then to plasticize the PLA/C30B blend. If all the components are incorporated

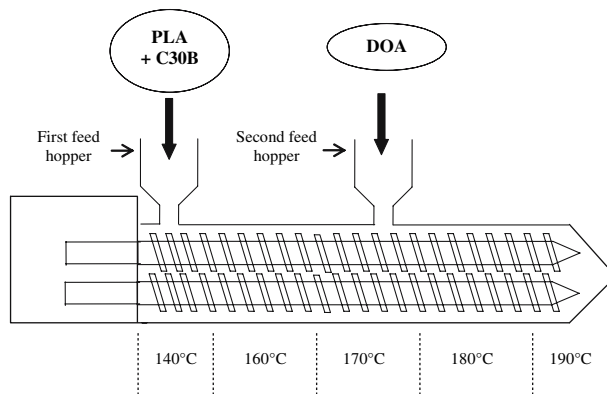


Fig. 1 Co-rotating extruder used to prepare pN4p

together, there is a competition between the PLA chains and the plasticizer to insert between the clay layers [24, 28]. The molecules of plasticizer are shorter than PLA chains, so they would insert easier between silicate layers. Then, plasticizer would be located between the layers and would be no more available to plasticize PLA.

Melt spinning

PLA, PLA nanocomposites and plasticized PLA nanocomposites are spin-drawn with the spinning device Spin-boy I from Busschaert Engineering. PLA filaments with 1%, 2% or 3% of C30B and 4% C30B/10% DOA (hereafter called N1_f, N2_f, N3_f, and pN4_f) are obtained. Pellets are first melted in a single screw extruder from 210 °C to 215 °C. Then melted PLA passes through two dies consisting of 40 channels with a diameter of 400 μm to obtain a multifilament continuous yarn, which is coated with Filapan CTC (blend of branched acid ester and branched

polyglycol), a spin finish supplied by Boehme. At last, the multifilament yarn is hot drawn between two rolls (see Fig. 2): the draw ratio (DR), which is the ratio between the rotation speeds of the feeding and the draw rolls, varies from 2 to 4. The speed of the first roll is maintained at 200 m/min, and the speed of the second roll varies from 400 m/min to 800 m/min. The temperature of the first roll is 70 °C, and the temperature of the second roll is 110 °C.

Knitting

Multifilament yarns made with PLA, PLA nanocomposites and plasticized PLA nanocomposites are knitted manually on a rectilinear machine gauge 8 (the structure of the knitted fabric is represented on Fig. 3). The multifilaments used are those, which have undergone the highest draw ratio (3.5 for PLA_f, N1_f and pN4_f, 3 for N2_f). These multifilaments have a fineness of approximately 1,600 dtex. Knitted fabrics with a surface weight of 1,000 g/m² and a thickness of 3 mm are obtained.

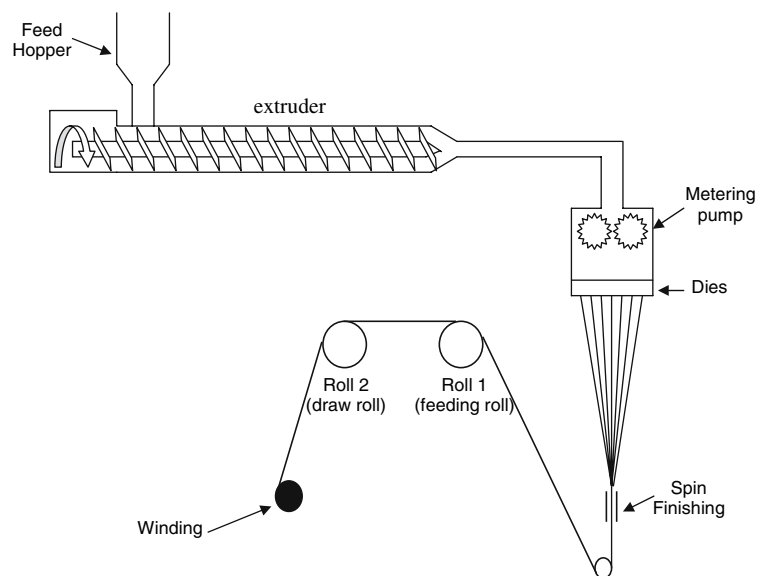
Investigation of the dispersion of C30B

The dispersion of C30B in N4_p, pN4_p and pN4_f is analysed using Wide-Angle X-ray Scattering (WAXS) and Transmission Electron Microscopy (TEM).

WAXS. The morphological analysis by X-ray diffraction was performed on a Siemens D5000 diffractometer using Cu(K_α) radiation (wavelength: 1.5406 Å) at room temperature in the range of $2\theta = 1.5^\circ\text{--}30^\circ$, by step of 0.04° and scanning rate of $2^\circ/\text{min}$.

TEM. Transmission electron micrographs were obtained with a Philips CM100 apparatus using an accelerator voltage of 100 kV. The samples were 70–80 nm thick and

Fig. 2 Principle of the spin-drawing machine



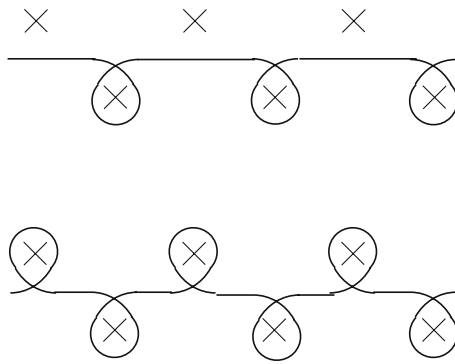


Fig. 3 Structure of the knit

prepared with a Reichert Jung Ultracut 3E, FC4E ultramicrotome cutting at $-130\text{ }^{\circ}\text{C}$.

Characterization of thermal properties of PLA pellets and fibers

Isothermal crystallization experiments were performed using a TA instruments DSC 2920. PLA pellet (5 mg) was placed in an aluminium pan and an empty pan was used as reference. The samples were heated up to $200\text{ }^{\circ}\text{C}$ to erase the thermal history. Then samples are cooled rapidly at $0\text{ }^{\circ}\text{C}$ to prevent crystallization. At last, samples are heated up to several isothermal temperatures lying between $80\text{ }^{\circ}\text{C}$ and $120\text{ }^{\circ}\text{C}$ ($10\text{ }^{\circ}\text{C}$ intervals when crystallization occurred), for at least 1 h to get a complete crystallization. At the end of the isotherm, samples are heated up to $200\text{ }^{\circ}\text{C}$ at $10^{\circ}\text{C}/\text{min}$ to observe the melting behavior. The relative crystallinity as a function of time can be monitored as follows:

$$X(t) = \frac{\int_0^t \frac{dH}{dt} dt}{\int_0^{\infty} \frac{dH}{dt} dt} = \frac{\Delta H_t}{\Delta H_{\infty}}$$

where $X(t)$ is the relative enthalpy at time (t), $\int_0^t \frac{dH}{dt} dt$ and ΔH_t are the crystallization enthalpy at time (t), $\int_0^{\infty} \frac{dH}{dt} dt$ and ΔH_{∞} are the crystallization at final time. It allows to determine $t_{1/2}$ of crystallization (time when $X(t) = 0.5$), and k , the overall kinetic constant by using Avrami equation [38]: $1 - X(t) = \exp(-kt^n)$ where n is the Avrami exponent.

The thermal characteristics of PLA pellets and fibers are investigated using the modulation option. In order to separate the glass transition and the relaxation phenomenon, the underlying rate used is $1^{\circ}\text{C}/\text{min}$, with an amplitude of $1\text{ }^{\circ}\text{C}$ and a period of 60 s. These parameters allow observing the glass transition in the reversing curve and the relaxation phenomenon in the non-reversing one. To observe the cold crystallization and the melting, the

underlying rate used is $5\text{ }^{\circ}\text{C}/\text{min}$ with an amplitude of $0.769\text{ }^{\circ}\text{C}$ and a period of 60 s. All experiments are carried out using helium as purge gas.

Characterization of the tensile properties of PLA fibers

The measurement of the tensile properties of PLA_f , N1_f , N2_f , N3_f and pN4_f have been carried out following the standard NF EN ISO 5079 on a tensile testing machine Zwick 1456, the cell force used is 10 N. All the tests have been made at standard atmosphere (the temperature is $20 \pm 2\text{ }^{\circ}\text{C}$ and the relative humidity is $65\% \pm 5\%$). The length between the clamps is 20 mm. All the results represent an average value of 50 tests.

Shrinkage of multifilaments yarn

The shrinkage of PLA and pN4 multifilaments has been measured at $70\text{ }^{\circ}\text{C}$ and $80\text{ }^{\circ}\text{C}$. The multifilaments (with an initial length L_0 of 1 m) are heated in hot air for 10 min without pre-tension. Then, the multifilaments are maintained at the ambient air during 20 min. Then a pre-tension of $0.4\text{ cN}/\text{tex}$ is applied during 30 s, and the final length (L_f) of the multifilaments is measured. The shrinkage (S) is given by the following equation:

$$S = \frac{L_0 - L_f}{L_0} \times 100$$

Thermal stability

TG analyses were performed using a TA 2050 Instruments at $10\text{ }^{\circ}\text{C}/\text{min}$ from $20\text{ }^{\circ}\text{C}$ to $850\text{ }^{\circ}\text{C}$ under flowing air ($50\text{ mL}/\text{min}$). Pellets (about 10 mg) were placed in open platinum pans. The precision on temperature measurements is $\pm 0.5\text{ }^{\circ}\text{C}$. Curves of the weight difference are also presented. These curves represent the difference between the experimental and theoretical curves. They are obtained as follows: MPLA(T) : TG curve of unfilled PLA, MC30B(T) : TG curve of C30B, MDOA(T) : TG curve of DOA, Mexp(T) : TG curve of the blend PLA/C30B/DOA, Mth(T) : theoretical TG curve calculated by linear combination between the TG curves of PLA, C30B and DOA if the sample is plasticized: $\text{Mth(T)} = x \cdot \text{MPLA(T)} + y \cdot \text{MC30B(T)} + z \cdot \text{MDOA(T)}$, $x + y + z = 1$ and x , y , z are, respectively, the mass percentage of PLA, C30B and DOA in the blend. For samples which are not plasticized, $z = 0$. The curve of weight difference, $\Delta(T)$, is calculated as follows: $\Delta(T) = \text{Mexp(T)} - \text{Mth(T)}$. This curve allows the observation of the possible interactions between the different components of a blend and the consequences on the thermal stability of the polymer.

Cone calorimetry by oxygen consumption

Knitted fabrics ($100 \times 100 \times 3 \text{ mm}^3$) were exposed in horizontal orientation in a FTT Cone Calorimeter, to an external heat flux of 35 kW/m^2 . This heat flux has been chosen because it represents common heat flux in mild fire scenario [39, 40]. All the experiments were repeated three times to check the reproducibility. The cone calorimeter was used to determine some fire properties, and particularly the rate of heat released (RHR), the total heat evolved (THE), which is the cumulated heat released, and time to ignition (t_{ig}).

Results and discussion

Study of the properties of PLA, PLA nanocomposites and plasticized PLA nanocomposite pellets

Dispersion of C30B in $N4_p$ and $pN4_p$

The structure of the nanocomposites has been observed by DRX. The DRX curves show that an intercalated structure

can be suggested (see Fig. 4). The characteristic peak of C30B located at 4.76° is shifted to lower 2θ values, i.e., 2.51° . So, by using the Bragg’s law, it is possible to calculate d , which is the interlayer space. For C30B and PLA/4% C30B, d is, respectively, 1.85 nm and 3.51 nm. It represents an increase of the interlayer space, d , of 1.66 nm. The structure of the nanocomposites has also been observed by TEM for $N4_p$ (see Fig. 5a, b). The dark lines represent the silicate layers of C30B which thickness is about 1 nm. On Fig. 5a, some silicate layers are fully delaminated and remain isolated. But some intercalated structures and tactoids can be observed as well (see Fig. 5b). So the structure of the nanocomposite seems to be exfoliated/intercalated. The dispersion of the other blends of PLA ($N1_p$, $N2_p$, $N3_p$) has not been studied. But we can expect that the dispersion of these blends is similar as that of $N4_p$.

The dispersion of C30B in $pN4_p$ has also been studied. Fig. 6a reveals that C30B is evenly dispersed in PLA. Some silicate layers are exfoliated even if some tactoids are still observed (see Fig. 6b). The XRD curve only gives a very weak diffraction peak around 6.37° (see Fig. 4). This weak peak is generated by a small quantity of a

Fig. 4 XRD curves of PLA, C30B, N4 and pN4

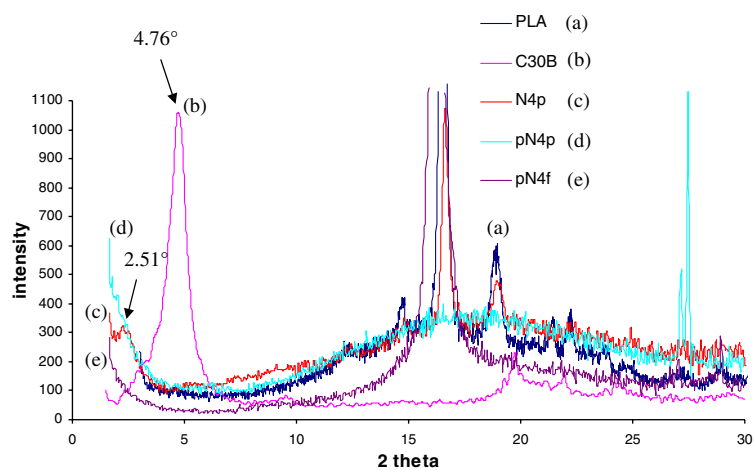


Fig. 5 TEM images of $N4_p$ at low (200 nm) and high (50 nm) magnification (a and b, respectively)

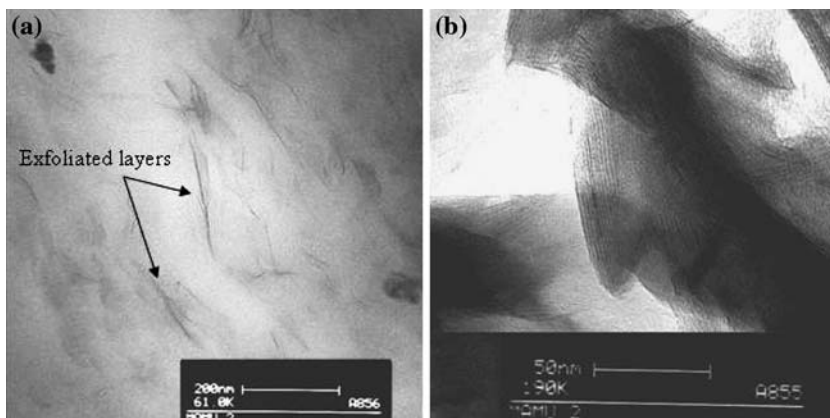
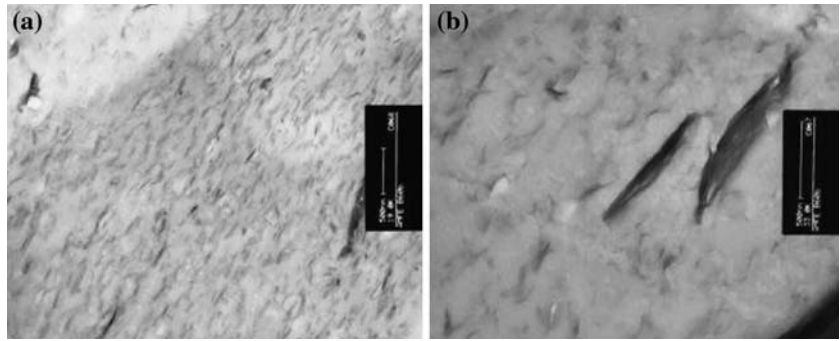


Fig. 6 TEM images of pN4p at low (500 nm) and high (100 nm) magnification (a and b, respectively)



by-product, which results from an oxidation of the double bond situated on the tallow alkyl chains of the organic modifier of C30B.

Crystallization kinetics

Three samples have been analysed: PLA_p, N2_p and N4_p. The results for the plasticized sample are not reported, the crystallization kinetics being too fast to be correctly monitored.

PLA is known to have a very slow crystallization rate. It was possible to monitor the development of the crystallization process only from 100 °C (see Fig. 7). Under this temperature, no crystallization occurred. But even if the isotherm is realized at 120 °C, the crystallization rate is still very slow. It is possible to accelerate it by blending PLA with a nucleating agent. Clays proved to display a strong influence on the crystallization rate of PLA, as well as on others polymers where they play the role of nucleating agent and promote crystallization [25, 27, 28, 41]. Only 2% in weight of C30B allows increasing the crystallinity rate. The silicate layers of C30B, which are delaminated can act as nucleating agents and promote the

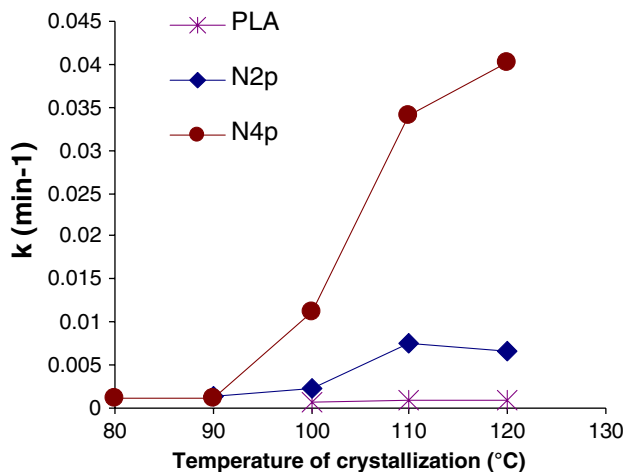


Fig. 7 Kinetic constant versus the temperature of crystallization

crystallization of the PLA macromolecules. It seems that this nucleation effect is increased when the quantity of C30B increases. Indeed, higher the quantity of C30B in a PLA matrix, higher quantity of silicate layers act as nucleating agent (see Fig. 7). At 120 °C, k is increased by a factor of 7 and 43 when PLA is filled with, respectively, 2% and 4% of C30B.

Effect of the plasticizer (DOA) on the thermal properties of PLA_p and N4_p

The plasticizer tends to decrease the glass transition temperature (T_g), the crystallization temperature (T_c) and the melting temperature (T_m) of PLA (see Fig. 8). It increases the molecular mobility, so a decrease in T_g can be observed. While T_g of PLA shows up at ca. 58.7 °C, T_g 's for PLA/10% DOA and pN4_p are, respectively, decreased to 40.8 °C and 44.2 °C. The plasticizer also facilitates the process of crystallization. For pristine PLA, the cold crystallization is not well defined. The cold crystallization is sharper and occurs at a lower temperature when PLA is plasticized. T_c of PLA is 124.3 °C and decrease to only 97.1 °C and 91.7 °C, respectively, for PLA/10% DOA and pN4_p. Accordingly, DOA promotes faster and more intensive crystallization. The crystallization enthalpy of unfilled PLA is only 8.0 J/g and this enthalpy increases up to 24.5 J/g and 21.6 J/g for PLA/10% DOA and pN4_p, respectively.

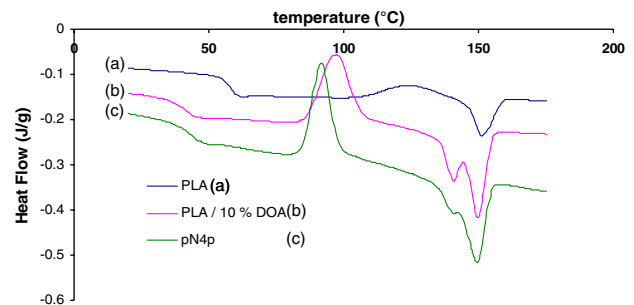


Fig. 8 Influence of plasticizer on the thermal properties of PLA and PLA/4% C30B

Thermal stability

TG curves of PLA, PLA nanocomposites, PLA/10% DOA, C30B and DOA are shown on Fig. 9. The first degradation of C30B occurs at about 220 °C. It corresponds to the degradation of the quaternary ammonium located between the silicate layers. The (plasticized) PLA and PLA nanocomposites degrade in one step. For N1_p, N2_p, N3_p and pN4_p, the difference can be hardly distinguished. A delay of the degradation is clearly observed for N4_p. To better estimate the influence of C30B on the thermal stability of PLA, the curves of temperature weight difference are represented on Fig. 9. For N1_p, N2_p, N3_p and N4_p, there is no interaction occurs from room temperature to 300 °C. However, a slight destabilization is observed between 200 °C and 330 °C only for N3_p. Then, a stabilization of the PLA matrix is observed. The range of the stabilization temperature varies depending on the quantity of C30B. The higher the quantity of C30B, the higher the range of stabilization temperature. For N4_p, the stabilization occurs between 280 °C and 370 °C. Then, a chaotic behaviour is observed around 370 °C. This behaviour is observed between stabilization and destabilization.

For pN4_p, stabilization is observed between 180 °C and 370 °C. Between 180 °C and 300 °C, it corresponds to the slower volatilization of the plasticizer when it is trapped in the polymer matrix. It is confirmed by the curve of temperature weight difference of PLA/10% DOA where stabilization occurs between 180 °C and 340 °C. Between 300 °C and 370 °C, it corresponds to the stabilization effect of the clay. This stabilization effect is less definite compared with N4_p because of a destabilization effect due to the plasticizer between 340 °C and 380 °C.

Study of the properties of PLA nanocomposites and plasticized PLA nanocomposite filaments

Dispersion of C30B in pN4_f

The structure of the pN4_f nanocomposite filaments (produced at DR = 4) has been observed by TEM. The dispersion is observed in the cross and longitudinal sections (see Fig. 10). The silicate layers are well dispersed, with very few aggregates. The images of the cross sections (Fig. 10a, b) show rather well defined dark lines (i.e., borders of the silicate layers), contrary to the images of the longitudinal sections (Fig. 10c, d) which show dark lines but also some

Fig. 9 TG and temperature dependent weight difference curves of PLA and (plasticized) PLA nanocomposites

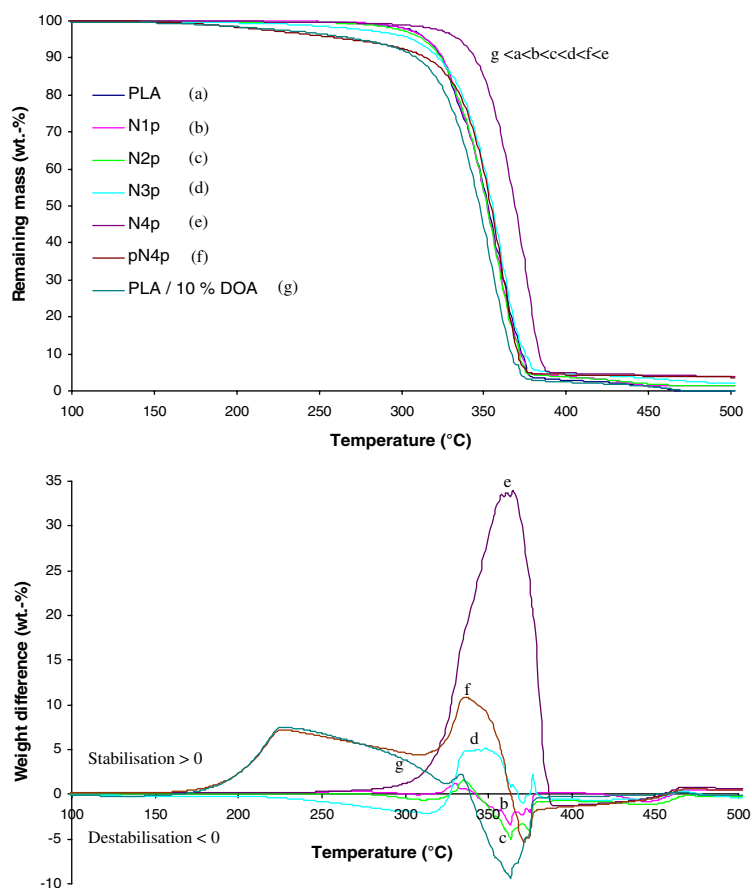
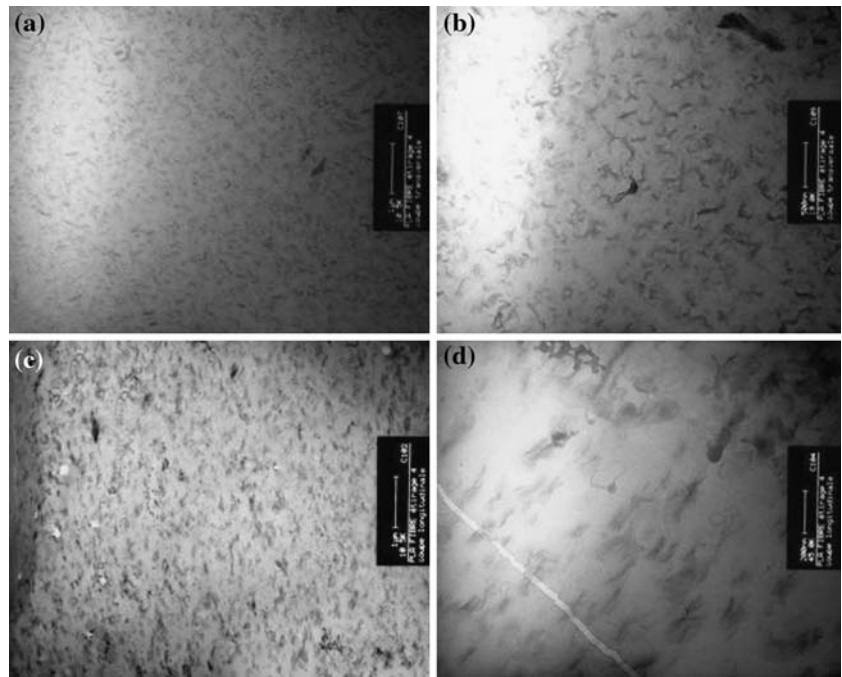


Fig. 10 TEM images of pN4_f (DR = 4). (a) and (b) represent cross sections at low and high magnification respectively. (c) and (d) represent longitudinal sections at low and high magnification, respectively



dark areas (i.e., surface of the silicate layers). So, an orientation of the silicate layers in the drawing direction may be assumed. The XRD curve of pN4_f (see Fig. 11) shows the disappearance of the characteristic peak of C30B. The good dispersion of C30B nanoplatelets (with only a limited amount of remaining aggregates) as observed on the TEM images might explain why no diffraction peak in the low 2θ angle range can be observed by XRD.

Tensile properties of PLA nanocomposite and plasticized PLA nanocomposite filaments

Table 1 summarizes the maximal draw ratio (DR), which was applied on the multifilaments before it broke. The higher the quantity of C30B, the lower the maximal DR. If the quantity of C30B is higher than 3% in weight, the PLA nanocomposite cannot be spun. This decrease in DR has a strong influence on the tensile properties of the filaments. To increase the quantity of C30B in the nanocomposite filaments, a plasticizer (DOA) has been added as third compo-

nent. This plasticizer has been used to apply higher DR and to obtain PLA nanocomposite filaments with higher elongation at break. Interestingly enough, PLA filaments filled with 4 wt.% C30B and 10 wt.% DOA could be produced. For the sake of comparison, some attempts to spin PLA/10% DOA filaments have been performed. But the multifilaments were not stable during the step of drawing, whatever the draw ratio studied (DR = 2 and 3). Accordingly, not enough filaments were obtained to be further knitted.

PLA used was first spun to study the influence of the processing conditions on the properties of the PLA filaments. It has been demonstrated that DR and the temperature of the draw roll have a strong influence on the tensile properties of PLA filaments. The tensile properties are optimum for a drawing temperature fixed at 110 °C and a DR of 3.5 [17]. PLA filaments with Young's modulus, tensile strength and elongation at break of 6.6 GPa, 442 MPa and 46.8%, respectively, are obtained.

The different nanocomposites were spun up to their maximal DR. The first observation is the strong decrease of

Fig. 11 XRD curves of PLA, C30B, and pN4_f (DR = 4)

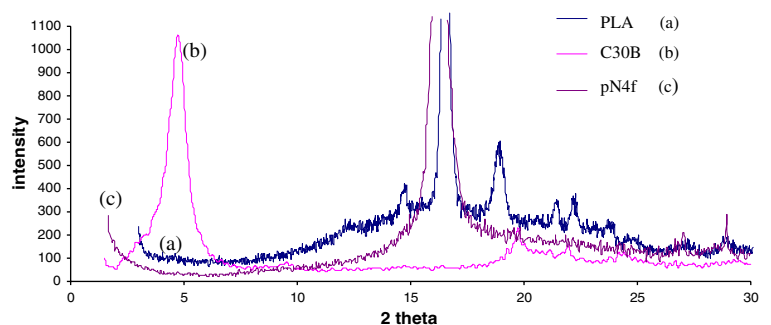


Table 1 Maximal DR applied

	Maximal DR applied
PLA	3.5
N1	3.5
N2	3
N3	2
N4	Not possible
pN4	4

the maximal DR possible to apply. The nanocomposite filaments were not able to undergo the same DR as PLA as soon as the quantity of C30B was higher than 1%. Only N1_p could be spun in the same conditions than PLA.

The Young’s modulus of nanocomposite PLA filaments decreases when the quantity of C30B increases. If the filaments are compared for a same DR, the Young’s modulus slightly decreases (cf. Fig. 12). This slight decrease is probably due to a faster degradation of the PLA matrix in presence of the organo-clay. During the degradation process of PLA, lactide and cyclic oligomers are generated [42]. These compounds are known to plasticize PLA, so they can trigger a slight decrease of the tensile properties. When comparing the Young’s modulus recorded for filaments based on each blend displaying the highest tensile properties, a strong decrease is observed at higher clay loading (see Table 2). Indeed, compared with the pristine PLA filaments, the Young’s modulus of N1_f, N2_f and N3_f decreases by 8.5%, 18.3% and 45.2%, respectively. This decrease is more likely explained by the difficulty for correctly drawing the PLA nanocomposites. So the molecular orientation cannot adequately occur, which ends up in lower Young’s modulus.

Usually, a plasticizer is used to decrease the rigidity of a material. It generally decreases the Young’s modulus and the tensile strength and increases the elongation at break.

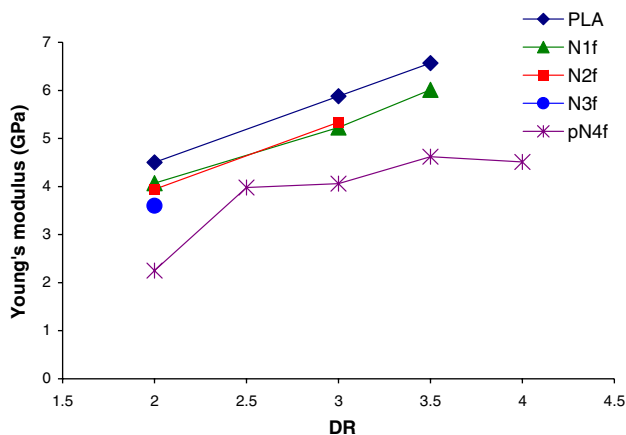


Fig. 12 Young’s modulus of filaments versus DR

N4 blend was not suitable to produce multifilaments as a result of its too low elongation behavior. When 10 wt.% DOA is added, multifilaments drawn up to 4 can be obtained. So, a plasticizer proved to be necessary to allow spinning of PLA filaments filled with 4 wt.% C30B with suitable elongation. But even if the pN4_f could be drawn up to DR of 4, the tensile properties remain lower than the properties recorded for unfilled PLA filaments. The Young’s modulus (see Fig. 12) is only 4.6 GPa, while a value of 6.6 GPa was measured for pristine PLA filaments.

A downward trend is also observed for the tensile strength (see Fig. 13). Compared with the unfilled PLA filaments, the tensile strength for N1_f, N2_f, N3_f and pN4_f (i.e., with the highest tensile properties) decreases by 1.3%, 28.9%, 43.4%, and 42.9%, respectively (see Table 2). Such a decrease for the tensile strength might again be explained by the impossibility of correctly drawing the PLA nanocomposites.

As far as the elongation at break of the filaments is concerned, it strongly decreases at higher C30B content (see Fig. 14). The elongation at break of N3_f is only 21.3%, even if the draw ratio is low (DR = 2). It proved to be lower than the elongation at break of pristine PLA filaments drawn at a DR of 3.5 (see Table 2). The elongation at break of pN4_f shows an unexpected behaviour with DR: the higher the DR, the higher the elongation at break. This behaviour is at the opposite of the unfilled PLA filaments behaviour where the elongation at break decreases at higher DR. This is probably due to an orientation effect of the silicate layers during the drawing process. At low DR, the silicate layers are not preferentially oriented and can represent some weak points within the drawn PLA matrix, which prevent a high elongation from being attained. At higher DR, a higher orientation of the silicate in the drawing direction can be assumed (see ‘‘Dispersion of C30B in pN4_f’’ section), so a decrease of these weak points.

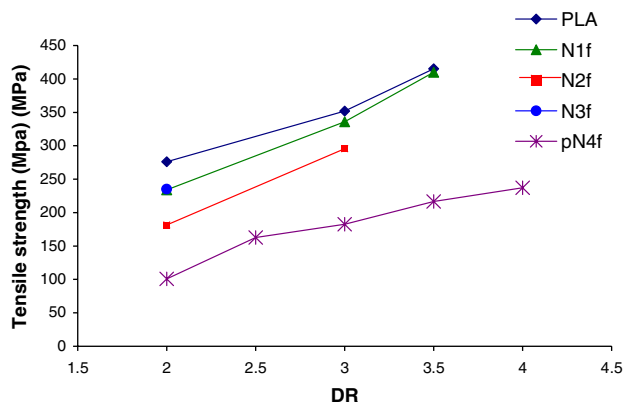


Fig. 13 Tensile strength of filaments versus DR

Table 2 Tensile properties of the filaments with the highest tensile properties for each blend

	PLA (DR = 3.5)	N1 (DR = 3.5)	N2 (DR = 3)	N3 (DR = 2)	pN4 (DR = 4)
Diameter (μm)	45.7	44.35	48.06	50.1	47.4
Young's modulus (GPa)	6.57	6.01	5.34	3.6	4.51
Tensile strength (MPa)	415	410	296	235	237
Elongation at break (%)	46.8	34.7	56.0	21.3	86.4

So, the consequence of blending PLA with C30B is the decrease of both the Young's modulus and the tensile strength of the filaments, which is mainly due to a strong decrease of the elongation of the filaments and the degradation of the PLA matrix. It is not possible to correctly draw the nanocomposite filaments. The so-obtained nanocomposite filaments show some low elongation at break as regards to pristine PLA-based filaments. This phenomenon has already been observed with nylon 6/clay nanocomposite fibers [43]. The silicate layers seem to prevent/refrain the molecular mobility of PLA macromolecules. So, the use of a plasticizer is necessary.

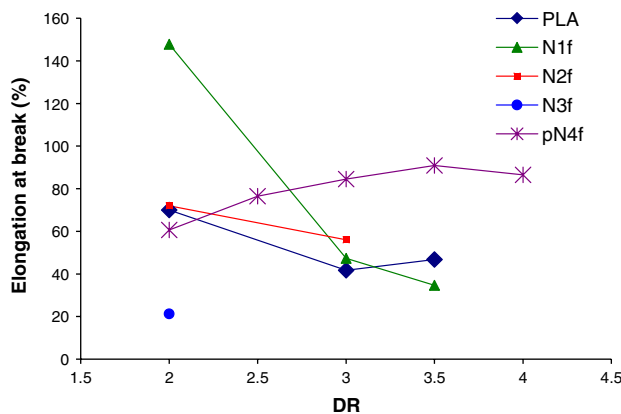
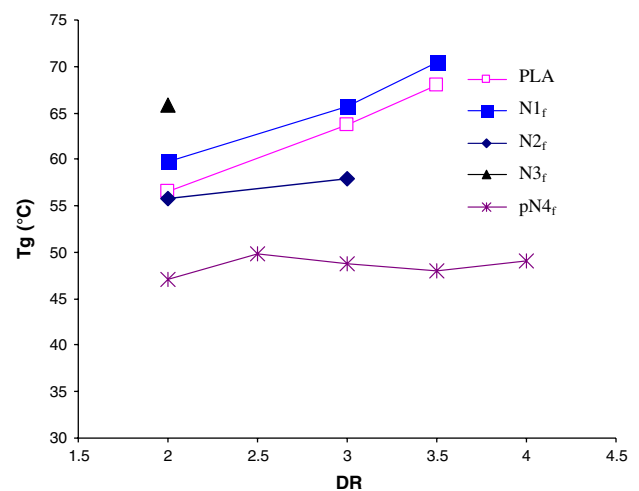
Thermal properties of PLA nanocomposite and plasticized PLA nanocomposite filaments

Glass transition temperatures of PLA and PLA nanocomposites filaments are represented in Fig. 15. For each kind of filaments, an increase of T_g is observed with DR. It is due to the increase of the degree of crystallinity with DR (see Fig. 16), which limits the molecular mobility, so the energy necessary to pass from the glassy state to the rubbery state is increased.

The N1_f, N2_f and N3_f have a T_g equal to or higher than the unfilled PLA filaments (except for N2_f with a DR of 3). PLA macromolecules intercalated between the silicate layers or in direct vicinity have their molecular mobility

and their flexibility restricted, which triggers an increase of T_g . The effect of the plasticizer is the decrease of T_g (see "Effect of the plasticizer (DOA) on the thermal properties of PLA_p and N4_p" section). The T_g of pN4_p is 44.2°C. When it is spun, a slight increase is observed. The filaments have a T_g between 47.1 °C (DR = 2) and 49.0 °C (DR = 4). So it represents only a 5 °C increase. This increase is more significant for the pristine PLA. The T_g of PLA pellets is 58.7 °C, and it increases up to 68.0 °C for PLA filaments (DR = 3.5). So it represents a ≈ 9.4 °C increase. The influence of the drawing process on T_g is less important when PLA is plasticized. Even if the drawing induces an orientation of the macromolecules and crystallization, the plasticizer increases the molecular mobility. So the increase of T_g of the PLA filaments due to the drawing is lower when the PLA is plasticized.

The N1_f, N2_f and N3_f are characterized by higher degrees of crystallinity as regards to the unfilled PLA filaments (see Fig. 16). Only PLA filaments with 1% and 2% of C30B drawn at low DR (2) have lowest degree of crystallinity. C30B increases the crystallization rate of PLA. As previously reported, silicate layers act as efficient nucleating agents and promote faster crystallization (see "Crystallization kinetics" section). The highest degree of crystallinity recorded for unfilled PLA filaments is 34% while it reaches 40.2% for N1_f. So, higher degrees of crystallinity are observed for PLA organo-clay nanocomposite

**Fig. 14** Elongation at break of filaments versus DR**Fig. 15** T_g of filaments versus DR

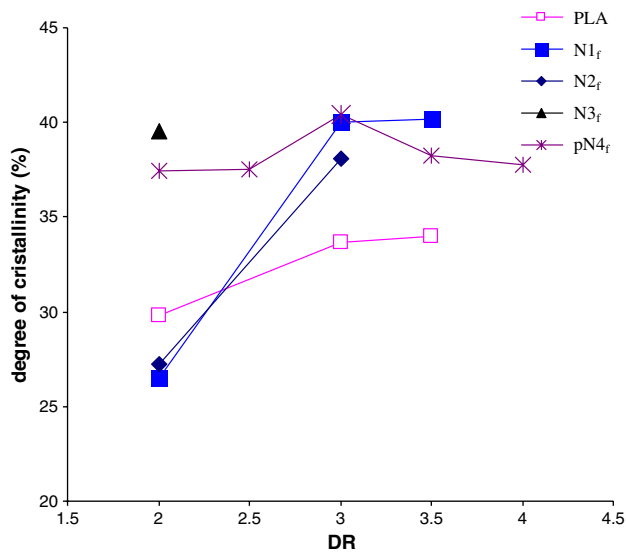


Fig. 16 Degree of cristallinity of filaments versus DR

filaments. The degree of cristallinity of pN4_f versus DR is also represented in Fig. 16. Higher degree of cristallinity is reached from lower DR(2). This high degree of cristallinity is due to the presence of C30B which increases the crystallization rate (see “Crystallization kinetics” section), but also to the presence of DOA which increases the molecular mobility of the PLA macromolecules (see “Effect of the plasticizer (DOA) on the thermal properties of PLA_p and N4_p” section). Whatever the investigated DR, the degree of cristallinity of pN4_f is around 37%, while it is only equal to 34% for unfilled PLA filaments at a DR of 3.5.

Reaction to fire of PLA nanocomposite filaments

The cone calorimeter is an efficient equipment to study the reaction to fire of a material. It allows to determine a large number of parameters which can describe the fire behavior of a material as the time to ignition (t_{ig}), the rate at which the heat is released (RHR), the total heat which is released (THR), the volume and toxicity of smoke produced. Three kinds of samples (PLA_f, N1_f and N2_f) were knitted to study the influence of the C30B content on reaction to fire. N3_f were not knitted because of the low tensile properties (see “Tensile properties of PLA nanocomposite and plasticized PLA nanocomposite filaments” section). The multifilament yarns were too weak and broke during knitting.

Figure 17 represents the RHR curves of PLA, N1 and N2 knitted fabrics. The time to ignition of PLA knitted fabric occurs at 76 s. When PLA is filled with C30B, t_{ig} slightly decreases. For N1 knitted fabric, t_{ig} is 75 s and for N2 fabric, it is 64 s. The decrease of t_{ig} of a polymer matrix filled with clay has already been observed [37, 44]. This decrease can be assigned to a partial degradation of the organic modifier during the melt blending and the melt

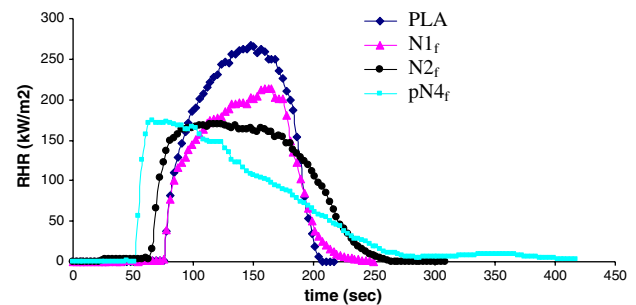
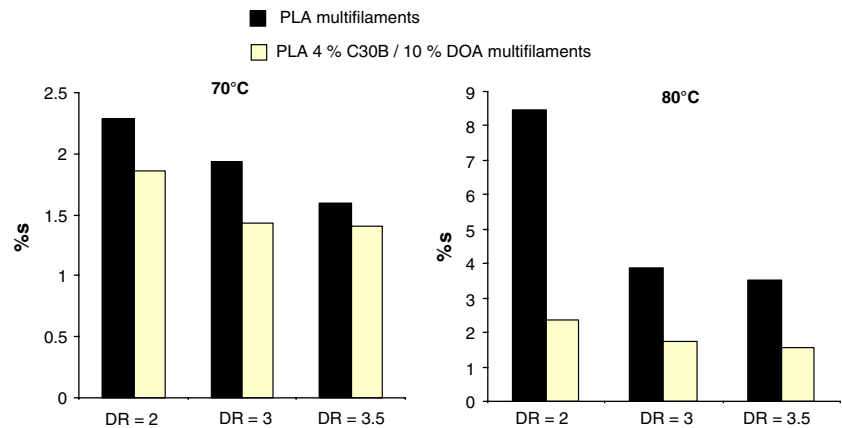


Fig. 17 RHR curves of PLA and PLA nanocomposites knitted fabrics

spinning. It can also be assigned to the fibrillation of the multifilament yarn. Short fibers are visible at the surface of the knitted fabrics. They can act as small matches leading shortening of the ignition time. For PLA knitted fabric, the maximal value for RHR is 265 kW/m². For N1 and N2 knitted fabrics, the maximal values are 213 kW/m² and 163 kW/m², respectively, which represents a decrease of 19% and 38%. The most noticeable effect is obtained for PLA filled with 2% of C30B. The RHR values reach a limit value (163 kW/m²) between 80 s and 180 s. This kind of plateau is not observed for unfilled PLA knitted fabrics. The decrease of RHR peak value can be explained by the formation of a char, which can be clearly seen when nanocomposite knitted fabrics are burning. This char has a double effect. It can prevent the small flammable molecules formed during degradation from being released, and prevent or at least refrain the oxygen molecules to diffuse into the material. The char can also protect the material from the heat by forming an insulating barrier.

The pN4_f have also been knitted to study the fire behavior using cone calorimeter. The RHR curve is presented in Fig. 17. The t_{ig} of pN4 knitted fabric is only 50 s, while it is 76 s for unfilled PLA knitted fabric. This decrease of t_{ig} is also observed for N2 knitted fabric. So, the higher the C30B content, the lower t_{ig} . But the plasticizer can also play a role in the decrease of t_{ig} . The TG curve (see Fig. 9) shows a volatilization of the plasticizer starting from 180 °C. It degrades more easily than PLA, which degradation occurs around 310 °C. So the volatilization of DOA can produce some gas, which can catch fire more easily. TG curves and cone calorimeter results can only be compared before t_{ig} , when a thermal oxidation of the material occurs. A strong decrease of the RHR peak can be noticed with a value equal to 173 kW/m². Compared to the maximal RHR value of pristine PLA knitted fabric (265 kW/m²), it represents a decrease of 34.7%. It is equivalent to the decrease observed between unfilled PLA and N2 knit fabrics. After the RHR peak, the RHR values decrease slowly. Some incandescence phenomena are observed at the end of the test, between 270 s and 420 s.

Fig. 18 Shrinkage of PLA and pN4 multifilaments



Shrinkage properties of plasticized PLA nanocomposite filaments

As expected, the shrinkage values increase with the temperature of the test (see Fig. 18). Interestingly, whatever the temperature of the test and the DR applied on the filaments, the shrinkages values for the pN4_f remain always lower as regards to the values of unfilled PLA filaments. This phenomenon has already been observed with some PET fibers modified with nanomaterials [45]. The silicate layers of C30B can decrease the molecular mobility of the macromolecules inserted between the silicate layers or in the vicinity. So these macromolecules are less sensitive to heat, and need higher temperature to shrink.

Conclusion

PLA organo-clay nanocomposites were prepared by melt blending, and particularly by twin-screw extrusion. Four types of nanocomposites, i.e., N1, N2, N3 and N4, containing, respectively, 1, 2, 3 and 4 wt.% of Cloisite® 30B (C30B), were extruded. The properties of these blends were firstly studied. TEM and XRD analyses showed a good dispersion of the C30B in the PLA matrix with an exfoliated/intercalated structure. It was also shown that C30B increases the crystallization rate and improves the thermal stability especially for PLA/4% C30B.

Then, these blends were spun with a melt-spinning drawing device. It was shown that problems to spin occurred for PLA filled with more than 2 wt.% of C30B. The elongation at break strongly decreases, so filaments with low tensile properties were obtained. So a fifth blend, using DOA as plasticizer (10 wt.%), was prepared and the resulting pN4 sample was extruded and successfully melt-spun drawn. The filaments obtained have better elongation properties, so they could be used to produce knitted fabrics.

Then, fire behavior of N1, N2 and pN4 knitted fabric was studied using a cone calorimeter. A strong decrease of the maximal RHR value, up to 38%, was obtained for N2 and pN4 fabric knits. It was shown that only 2 wt.% of C30B was enough to improve the fire behavior of the fabric knit. PLA organo-clay nanocomposite is a very promising route to improve the fire behavior of a textile structure. It allows obtaining PLA knitted fabric with flame retarding properties.

Acknowledgements The authors are very grateful to Interreg III ‘‘France-Wallonie’’, Région Wallonne, Région Nord Pas de Calais and European Union (FEDER) for the financial support in the frame of interregional project MABIOLAC. SMPC thanks the Belgian Federal Government Office of Science Policy (SSTC-PAI 5/3) for general support and is much indebted to both ‘‘Région Wallonne’’ and the European Commission ‘‘FSE and FEDER’’ for financial support in the frame of Phasing-out Hainaut: Materia Nova.

References

1. Agrawal AK, Bhalla R (2003) *J Macromol Sci Part C Polym Rev* C43:479
2. Postema AR, Luiten AH, Pennings AJ (1990) *J Appl Polym Sci* 49:1265
3. Postema AR, Luiten AH, Oostra H, Pennings AJ (1990) *J Appl Polym Sci* 49:1275
4. Tsuji H, Ikada Y, Hyon S-H, Kimura Y, Kitao T (1994) *J Appl Polym Sci* 51:337
5. Horacek I, Kalisek V (1994) *J Appl Polym Sci* 54:1751
6. Horacek I, Kalisek V (1994) *J Appl Polym Sci* 54:1759
7. Eling B, Gogolewski S, Pennings AJ (1982) *Polymer* 23:1587
8. Leenslag JW, Pennings AJ (1987) *Polymer* 28:1695
9. Schmack G, Jehnichen D, Vogel R, Tändler B, Beyreuther R, Jacobsen S, Fritz H-G (2001) *J Biotech* 86:151
10. Schmack G, Tändler B, Optiz G, Vogel R, Komber H, Häußler L, Voigt D, Weinmann S, Heinemann M, Fritz H-G (2004) *J Appl Polym Sci* 91:800
11. Mezghani K, J.E Spruiell (1998) *J Polym Sci Part B Polym Phys* 36:1005
12. Schmack G, Tändler B, Vogel R, Beyreuther R, Jacobsen S, Fritz H-G (1999) *J Appl Polym Sci* 73:2785
13. Takasaki M, Ito H, Kikutani T (2003) *J Macromol Sci Part B Phys* 42: 57

14. Fambri L, Pegoretti A, Fenner R, Incardona SD, Migliaseri C (1997) *Polymer* 38:79
15. Cicero JA, Dorgan JR, Dec SF, Knauss DM (2002) *Polym Degrad Stab* 78:95
16. SolarSKI S, Ferreira M, Devaux E (2005) *Polymer* 46:11187
17. SolarSKI S, Ferreira M, Devaux E (2006) *J Textile Instit* (accepted)
18. Alexandre M, Dubois P (2000) *Mat Sci Eng* 28:1
19. Sinha Ray S, Okamoto M (2003) *Prog Polym Sci* 28:1539
20. Morgan AB, Gilman JW (2003) *J Appl Polym Sci* 87:1329
21. Bourbigot S, Vanderhart DL, Gilman JW, Awad WH, Davis RD, Morgan AB, Wilkie C, (2003) *J Polym Sci Part B Polym Phys* 41:3188
22. Krikorian V, Pochan DJ (2003) *Chem Mater* 15:4317
23. Wu T, Chiang MF (2005) *Polym Eng Sci* 45:1615
24. Paul MA, Alexandre M, Degée P, Henrist C, Rulmont A, Dubois P (2003) *Polymer* 44:443
25. Pluta M, Galeski A, Alexandre M, Paul M-A, Dubois P (2002) *J Appl Polym Sci* 86:1497
26. Nam PH, Fujimori A, Masuko T (2004) *J Appl Polym Sci* 93:2711
27. Di Y, Iannace S, Di Maio E, Nicolais L (2005) *J Polym Sci Part B Polym Phys* 43:689
28. Pluta M (2004) *Polymer* 45:8239
29. Paul MA, Alexandre M, Degée P, Calberg C, Jérôme R, Dubois P (2003) *Macromol Rapid Commun* 24:561
30. Paul MA, Delcourt C, Alexandre M, Degée P, Monteverde F, Rulmont A, Dubois P (2005) *Macromol Chem Phys* 206:484
31. Martin O, Avérous L (2001) *Polymer* 42:6209
32. Baiardo M, Frisoni G, Scandola M, Rimelen M, Lips D, Ruffieux K, Wintermantel E (2003) *J Appl Polym Sci* 90:1731
33. Ljungberg N, Wesslen B (2002) *J Appl Polym Sci* 86:1227
34. Younes H, Cohn D (1988) *Eur Polym J* 24:765
35. Labrecque LV, Kumar RA, Dave V, Gross RA, Mc-Carthy SP (1997) *J Appl Polym Sci* 66:1507
36. Jacobsen S, Fritz HG (1999) *Polym Eng Sci* 39:1303
37. Bourbigot S, Devaux E, Flambard X (2002) *Polym Degrad Stab* 75:397
38. Avrami M (1939) *J Chem Phys* 7:1103
39. Babrauskas V (1982) Development of cone calorimeter-a bench scale, rate of heat release based on oxygen consumption: NBS-IR 82-2611. US Nat Bur Stand, Gaithersburg
40. Babrauskas V (1984) *Fire Mater* 8:81
41. Sinha S Ray, Okamoto M (2003) *Macromol Rapid Commun* 24:815
42. Kopinke F-D, Remmle M, Mackenzie K, Möder M, Wachsen O (1996) *Polym Degrad Stab* 53:329
43. Yoon K, Polk MB, Min BG, Schiraldi DA (2004) *Polym Intern* 53:2072
44. Gilman JW (1999) *Appl Clay Sci* 15:31
45. Xiao W, Yu H, Han K, Yu M (2005) *J Appl Polym Sci* 96:2247